



Wide Band Pulse Phase Resolved Spectroscopy with BeppoSax.

A. Santangelo^a, S. Del Sordo^a, S. Piraino^a, A. Segreto^a, G. Cusumano^a, D. Dal Fiume^b, M. Orlandini^b, A.N. Parmar^c

^aIstituto di Fisica Cosmica ed Applicazioni dell'Informatica, C.N.R.,
Via Ugo La Malfa 153, 90146 Palermo

^bIstituto Tecnologie e Studio Radiazioni Extraterrestri, CNR, Via Gobetti 101, 40129 Bologna, Italy

^cAstrophysics Division, Space Science Department of ESA, ESTEC
Keplerlaan 1, 2200 AG Noordwijk, The Netherlands

Broad-band observation of galactic X-ray binary pulsars is one of the main scientific goal of the *BeppoSAX* mission. In this framework a key role is played by Pulse Phase Resolved Spectroscopy. In the paper we present some preliminary results on both phase-resolved spectra and pulse profile evolution with energy on two sources of this class, Cen X-3 and Her X-1.

1. INTRODUCTION

Observation and studies of galactic X-ray sources and among them of accreting strongly magnetized neutron stars in binary systems is one of the main guideline of the *BeppoSAX* scientific Core Program. In this framework a key role is played by Pulse Phase Resolved Spectroscopy. Indeed, *BeppoSAX* has this unique capability: to obtain, combining simultaneous observations of its Narrow Field Instruments (NFIs), spectra for different segments of the pulse phase, over an unprecedented broad energy band (from the fraction of keV up to 200 keV) with good energy resolution and statistics. This has a great impact in three areas: 1) phase dependence of the primary spectral component; 2) phase dependence of the fluorescence emission, typically the iron line; 3) phase dependence of high energy features, typically Cyclotron Resonant Scattering Features (CRSFs).

Aim of this paper is to show some recent results from *BeppoSAX* on two well known X-ray Binary Pulsars, Cen X-3 and Her X-1. As far as concerns Cen X-3, after discussing the evolution of pulse profile with the energy, we will report some results on the phase dependence of the iron line parameters. We will, then, conclude with the study of the phase averaged spectrum observed by *BeppoSAX* NFIs in the post-egress

high state of the source reporting the detection of an absorption-like feature that we interpret as a cyclotron feature.

Some preliminary analysis of pulse phase resolved spectra of Her X-1, with main emphasis on the variation with phase of Cyclotron feature, will be, also, discussed in the paper.

2. CEN X-3

Centaurus X-3 was the first binary pulsar to be discovered in the X-ray sky [1,2]. The system contains a neutron star which exhibits a pulse period of 4.8 sec while orbiting a highly reddened O-type companion, [3], every 2.09 days. Although a strong stellar wind emanates from the companion, due to the behaviour of its optical light curve Cen X-3 is thought to be powered by an accretion disk fed by Roche Lobe overflow. Moreover the discovery of QPOs from the source, [4], further implies the presence of an accretion disk. The X-ray luminosity of the system has been found to vary, from a high luminosity to a low luminosity state, by a factor of 8 on a timescale of months. Also pulse shape is variable changing both with the energy and luminosity ([5] and references therein).

BeppoSAX, the Italian-Dutch Mission for X-ray Astronomy [6], observed Cen X-3 with the

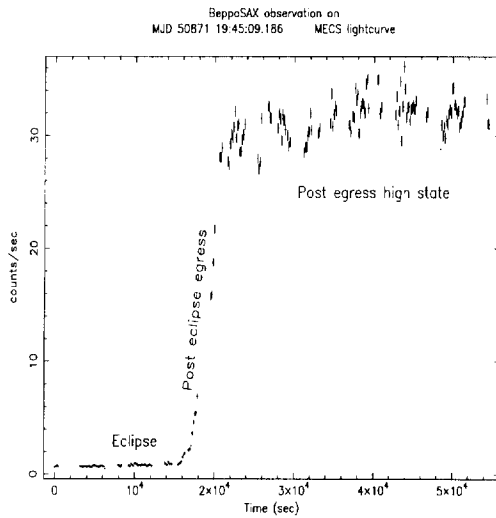


Figure 1. Cen X-3 background subtracted light curve observed, during the AO1 pointing, in the *BeppoSAX* MECS (2–10 keV).

Narrow Field Instruments ([8,7,9,10]) twice. The first time the source was observed on August 14th, 1996 in the framework of Science Verification Phase Program. It was found, assuming a distance of 8 Kpc, at a luminosity level of $4.6 \cdot 10^{36}$ erg s^{-1} . Data from this observation are not discussed here and will be the subject of a different paper [11]. The source was observed again by the NFIs on February 17th, 1997 in the framework of the AO1 program, covering the orbital phase from 0.0 (mid-eclipse) to 0.3. As can be seen in Fig. 1, where the light curve observed by the Medium Energy Concentrators Spectrometers (MECS) is shown, during this second observation part of the eclipse, the post-eclipse egress and the post-egress high luminosity state were monitored. Unfortunately, out of the eclipse, the LECS instrument was off. Assuming again a distance of 8 Kpc, the X-ray luminosity of the source was, during this second observation, at a level of $4.3 \cdot 10^{37}$ erg s^{-1} (in the 2–10 keV band).

2.1. Pulse Profiles.

Pulse Profiles of Cen X-3 in six different energy bands relative to high post-egress state are shown

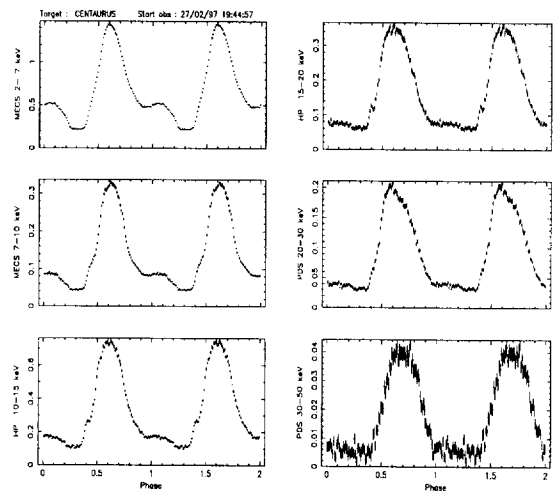


Figure 2. Cen X-3 pulse profiles in six different energy ranges and relative to 0.2 – 0.3 orbital phase (post-egress high state).

in Fig. 2.

Pulse profile clearly evolve with the energy. At lower energies, below 15 keV, it shows a "single main" peak with a sharp rise and a more gradual decline ending in a shoulder that is usually defined as the "subsidiary" peak. Three peculiar phase segments can, then, be defined: the "single main" peak, the "subsidiary" peak (separated 180 deg from the main peak) and a third phase segment that we define interpulse. At higher energies (above 15 keV) the subsidiary peak is almost suppressed and only the main single peak is observed. It is also interesting to note that in the 10–15 keV energy range a small shoulder on the trailing edge is clearly observed by the High Pressure Gas Scintillation Proportional Counter (HPGSPC).

The "single peak" structure is not unique. A rarely observed double peaked (not strongly asymmetric) profile has been reported in a few occasions[5]. Nagase et al. suggested a possible dependence of pulse profiles on luminosity as in the case of EXO 2030+375[13]. In that case

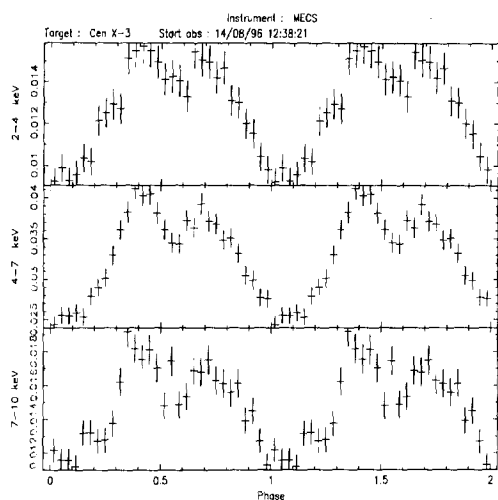


Figure 3. Cen X-3 pulse profiles in three different energy ranges during the Science Verification Phase low luminosity observation of the post-egress high state. A more complex structure appears.

the luminosity dependence of the pulse profile is explained with the change of emission from fan beam to pencil beam, due to a different structure of the accretion column. As we, already said, during the Science Verification Phase *BeppoSAX* observed Cen X-3 while the source was in the post-egress orbital phase but at a very different luminosity level. Pulse profiles as a function of the energy are reported in Fig. 3. A, complex, more double peaked structure is clearly detected.

2.2. Pulse Phase Spectroscopy of the iron line.

The detection, in the *Ginga* data of pulsed iron line emission from Cen X-3 was reported by Day et al. in 1993 [12]. The discovery of such a pulsation had, of course, a great impact in settings the constraints that models of iron line emission mechanism and geometry must satisfy.

In order to search for pulse phase dependencies in the spectrum, we integrated the spectra in 20 pulse phase bins, each with an effective integration time of about 1ksec. Data were fitted with a

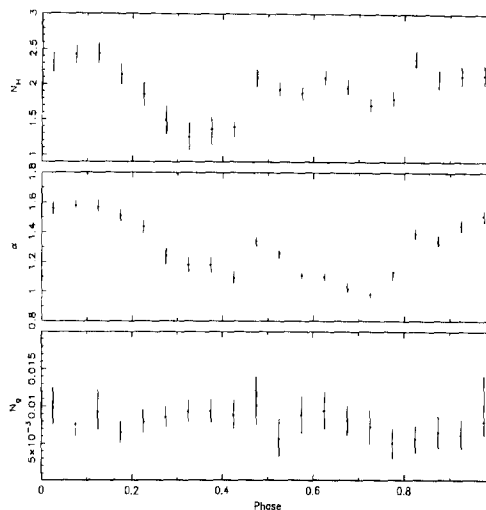


Figure 4. Absorbing column, N_H , spectral index α , and iron line intensity N_g as a function of the pulse phase. Errors on a single parameter are at 90% confidence level in χ^2_ν variation.

single model comprising a power law, a gaussian shape iron line and the photoelectric absorption. Over the 2–10 keV range the power law provides a good modelling of the continuum and good fits ($\chi^2_\nu \simeq 1$) are obtained at each phase bin. The relevant best fitting parameters, absorption column, photon index and intensity of the line are shown in Fig. 4 as functions of the pulse phase.

Errors on a single parameter are at 90% confidence level in χ^2_ν variation. Both the absorption column N_H and spectral index α vary with the phase, the "subsidiary peak" being the softest part of the pulse profile, while the "main" peak shows a harder spectrum. The average values of iron line intensity vary less than 40% and however well inside the 90% error bars. Moreover, the absorption column N_H and the iron line intensity are not in phase with each other. This result is different from what *Ginga* observed in 1992 and could be related to the difference in luminosity between the two observations.

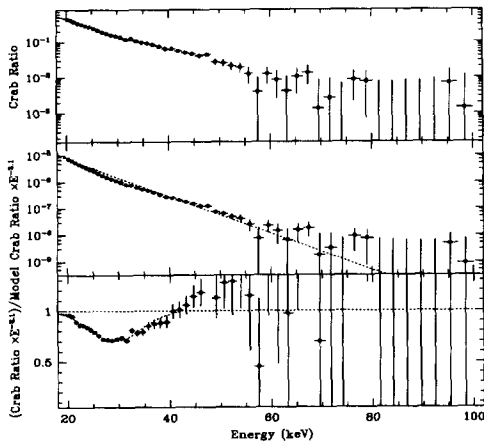


Figure 5. Upper panel: Ratio between the Cen X-3 and the Crab count rate spectra. Middle panel: the ratio multiplied $E^{-2.1}$. Deviations from the continuum are present around 28 keV. Lower panel: the middle panel curve divided by the best fit continuum from the broad band fit.

2.3. The Phase Averaged Spectrum.

It has been an open question if any cyclotron resonant scattering feature is present or not in the spectrum of Cen X-3 [5,14]. As a first step, in order to search for features in the phase averaged spectrum we considered the ratio between the Cen X-3 and the Crab spectra measured by the Phoswich Detection System (PDS) instrument. This ratio, shown in panel a of Fig. 5, is largely independent of uncertainties in effective area calibration. [17,16].

In order to amplify any deviation from the smooth continuum, in panel (b) of Fig. 5, we report the count rate ratio multiplied by the functional form of the Crab nebula, a featureless power law with spectral index $\alpha = 2.1$ in this energy range. Indeed, a clear deviation of the continuum is observed. The shape of this feature can be amplified dividing the count rate ratio by the continuum obtained with the best fit model (described below). In the lowest panel (c)

of Fig. 5, a clear absorption feature centred at 28.5 keV emerges. Fitting the data with a simple Gaussian in absorption, we get $E_{crsf} = 29.3 \text{ keV}$, $\sigma_{crsf} = 5.1$, for a $\chi^2_\nu \simeq 1.9(22)$.

To extract physical information, however, we searched for this feature, fitting the phase averaged spectrum of the post-egress high state with different theoretical models (Fig. 6). The only continuum model which came close to describe the observed spectrum was a broken powerlaw with an exponential turn-over at high energies (see [18], for the functional form). Also the photoelectric absorption [19] and a contribution from a gaussian shape line for cold iron were included the continuum. Regardless of the continuum used some persistent feature was present in the residuals. This suggested us to include a cyclotron resonant scattering line in the model. We did introduce the absorption-like line in two different ways: 1) Coupled Lorentzian lines [14] 2) a Gaussian line in absorption [21], [17]. The relevant best fit parameters for the two cases are reported in Tab1. In both cases an absorption-like feature is found at $E_{cyc} \simeq 28 \text{ keV}$. Interpreting this feature as due to cyclotron resonance scattering the magnetic field strength at the surface of the neutron star can be calculated from the line centroid using $E_{cyc} = 11.6 B_{12} \cdot (1+z)^{-1} \text{ keV}$ where z is the gravitational redshift. In the case of Cen X-3 a magnetic field of about $2.4 \cdot (1+z)^{-1} \cdot 10^{12} \text{ Gauss}$ is inferred. If we consider $z \simeq 0.3$ the strength of magnetic field is about $3.2 \cdot 10^{12} \text{ Gauss}$. This value is in good agreement with what reported in [20] on the basis of beat frequency mass accretion model.

3. HER X-1

The Low Mass eclipsing X-ray binary Her X-1 [22], is one of the most observed and studied X-ray pulsars in the sky. Beside a pulse period of 1.24 sec. and an orbital period of 1.7 days, the source exhibits a 35 day X-ray intensity cycle which manifests itself as a 10 day main on-state followed by a 5 day secondary short-on state during which the intensity of the source is a factor of 3 fainter. The two on-states are separated by periods of relatively low flux. This modulation has

Table 1
Best Fit Spectral Parameters for phase averaged spectrum of Cen X-3

Parameter		Value		
		No Line	Gaussian	Lorentzian
N_H	10^{22} cm^{-2}	1.92 ± 0.02	1.93 ± 0.02	1.92 ± 0.02
α_1		1.22 ± 0.01	1.22 ± 0.01	1.22 ± 0.01
α_2		3.23 ± 0.12	2.8 ± 0.12	2.38 ± 0.13
E_{break}	(keV)	17.5 ± 0.3	17.3 ± 0.3	18.1 ± 0.4
E_{cutoff}	(keV)	11.9 ± 0.2	12.2 ± 0.2	12.6 ± 0.2
$E_{folding}$	(keV)	15.0 ± 0.9	13.4 ± 0.9	12.1 ± 0.8
E_{CRF}	(keV)	28.5 ± 0.5	27.8 ± 0.5
σ_{CRF}	(keV)	3.1 ± 0.8
$Width_{CRF}$	(keV)	6.0 ± 2
χ^2_{ν}		1.87 (312)	1.4 (310)	1.28 (310)

NOTE — All quoted errors represent 90% confidence level for a single parameter.

N_H is the absorbing column, $\alpha_{1,2}$, power laws indexes, E_{break} , the break energy between the two power laws, E_{cutoff} is the cut-off energy of the exponential roll-off, $E_{folding}$ is the folding of the exponential roll-off, E_{CRF} is the position of the cyclotron line, σ_{CRF} is the gaussian width while $Width_{CRF}$ is the width of the Lorentzian.

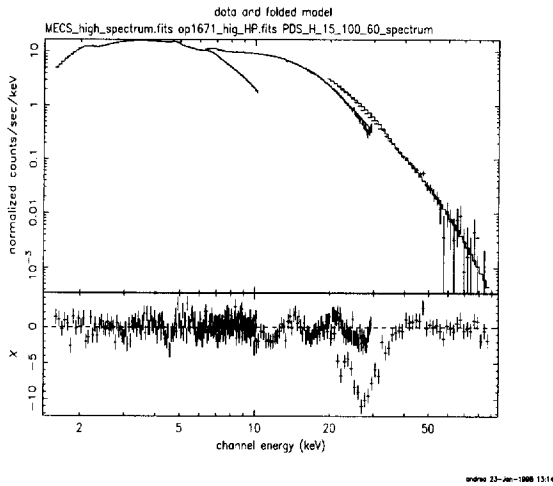


Figure 6. The broad band post-egress high state spectrum of Cen X-3 observed by the *BeppoSAX* NFIs. Upper panel: count rate spectrum and best fitting continuum model. Lower panel: the gaussian in absorption has been set to zero and residuals from the Gaussian best-fit model are shown.

been explained with a tilted precessing accretion disk that periodically obscures the line of sight toward the neutron star [25]. Her X-1 was the first pulsar from which a cyclotron scattering feature was detected [26,27]. The feature has been, since then, extensively studied and discussed in terms of either an emission line at 45 keV or an absorption line at 35 keV. Variation of spectral parameters with the pulse light curve have also been discussed by Soong et al., [21], and results seem to make the absorption interpretation more likely. The NFIs onboard *BeppoSAX* observed Her X-1 on July, 24th, 1996, during the Science Verification Phase, covering two full orbital cycles near the maximum of the main-on state.

3.1. Pulse Profiles

Pulse profiles from 0.1 up to 100 keV have been already presented and discussed by Dal Fiume et al. [17] and will not be reported here. Major changes are present below 1 keV, where the transition from a broad sinusoidal shape to a more peaked structure can be interpreted as reprocessing from the inner part of the accretion disk, and above 10 keV where the pulse profile is much less structured. The pulse profile, however, evolves with the energy in the entire *BeppoSAX*

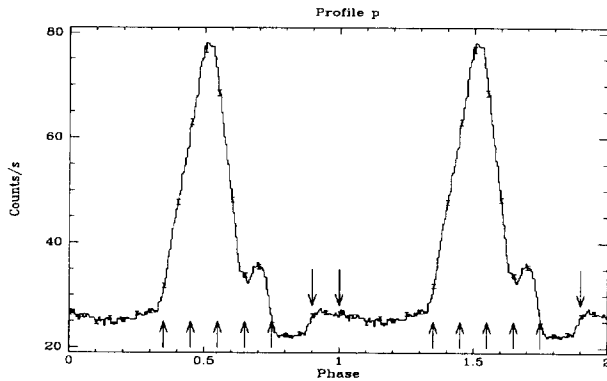


Figure 7. Her X-1 pulse profile as observed by the MECS in the 2-10 keV energy range. The pulse light curve has been divided in 7 phase segments, numbered from left to right.

band, indicating that there is a dependence on the phase of the spectrum.

3.2. Spectral Analysis

The broad band phase averaged spectrum of Her X-1 as observed by *BeppoSAX* ([23,24]), is quite complex. Three different components are evident in the continuum, 1) a low energy excess modelled as 0.1 keV blackbody; 2) a power law; 3) a higher energies exponential cut-off. Superimposed in the continuum, Fe K and L emission line at 1.0 and 6.5 keV respectively and a cyclotron absorption feature at 40 keV are detected.

In order to study the dependence of line parameters on pulse phase, the pulse light curve has been divided in 7 phase segments as shown in Fig. 7

PDS Count rate spectra normalized respect to the Crab spectra and multiplied by The Crab spectral functional form have been, then, obtained for all the phase segments and are shown in Fig. 8.

Although results are quite preliminary a strong dependence on the pulse phase of the line parameters is clearly evident, the line being larger and more deeper around the peak of the pulse. A more detailed and quantitative analysis is, of

course, on the way.

REFERENCES

1. R. Giacconi et al., *ApJ*, 167, L67, 1971
2. Schreier et al., *ApJ* 172, L179, 1972
3. Krzeminski, W., *ApJ*, 192, L135, 1974
4. Takeshima T et al., *PASJ* 43, L43-L50, 1991
5. F. Nagase et al., *ApJ*, 396 1992
6. G. Boella et al., *A&AS*, 122, 299, 1997
7. G. Boella et al., *A&AS*, 122, 327, 1997
8. A. N. Parmar et al., *A&AS*, 122, 309, 1997
9. G. Manzo et al., *A&AS*, 122, 341, 1997
10. F. Frontera et al., *A&AS*, 122, 357, 1997
11. S. Del Sordo et al., these Proceedings
12. C. Day et al., *ApJ*, 408, 656, 1993.
13. A. Parmar et al *ApJ*, 338, 373, 1989.
14. T. Mihara, PhD thesis, 1995.
15. S. Piraino et al, *A&A*, in preparation
16. M. Orlandini et al., these Proceedings
17. D. Dal Fiume et al., these Proceedings
18. Xspec User's Manual V9.0.
19. R. Morrison and D. McCammon, *ApJ*, 270, 119, 1983
20. G. Audley et al., *ApJ*, 457, 397, 1996.
21. Y. Soong et al., *ApJ* 348, 641, 1990.
22. H. Tananbaum et al., *ApJ*, 174, L143, 1972.
23. D. Dal Fiume et al., Accepted in *A&A*, 1997
24. T. Oesterbroek et al., *A&A*, 327, 215, 1997
25. D. Gerend and P.E. Boynton, *ApJ* 235, 999, 1980.
26. J. Trümper et al., *ApJ*, 219, L105, 1978.
27. T. Mihara et al., *Nature*, 346, 250, 1990.
28. N. E. White et al., *ApJ*, 270, 711, 1983

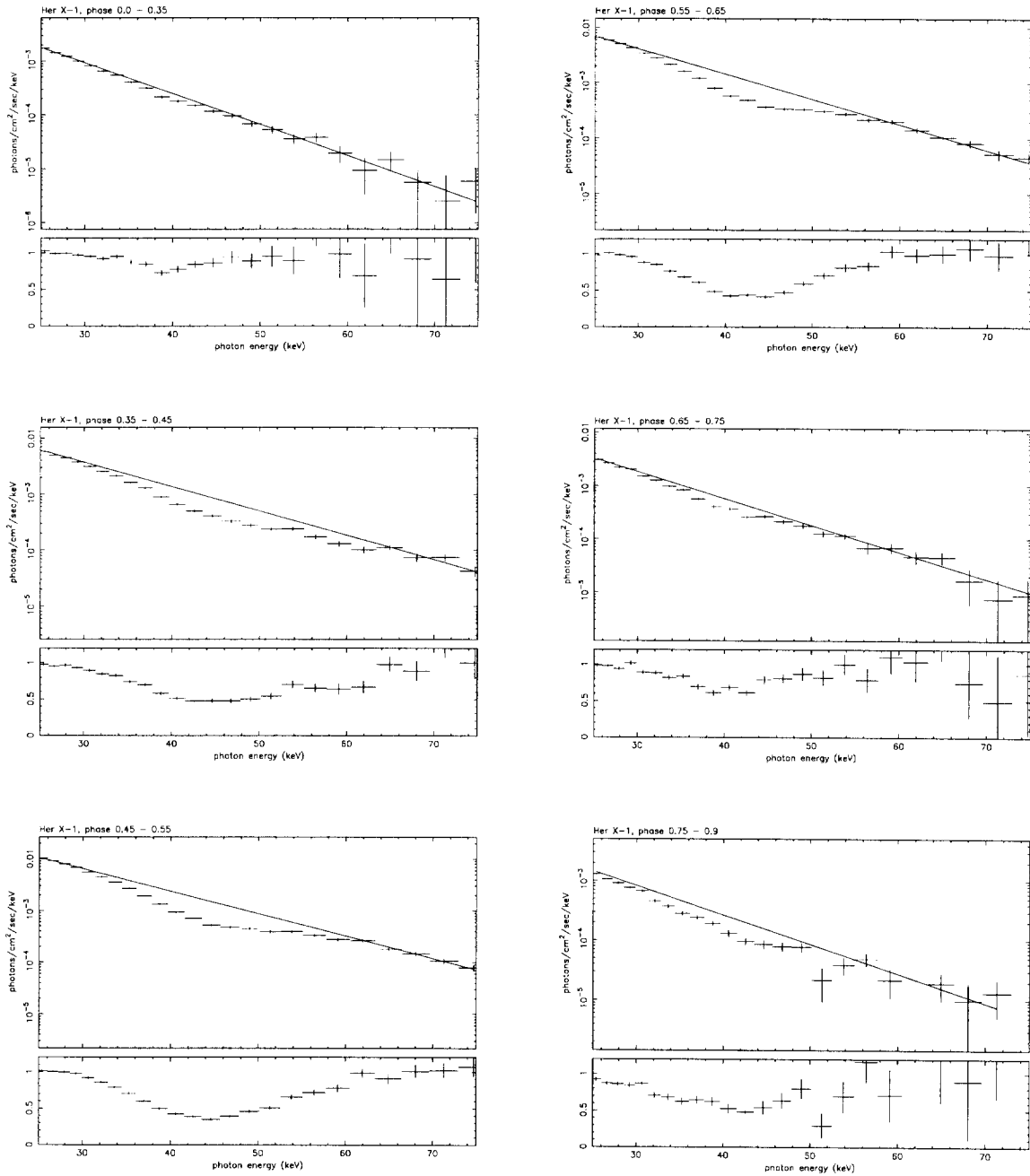


Figure 8. In the Upper panels, the ratios of the PDS count rate spectra of Her X-1 and the Crab Nebula, multiplied by $E^{-2.1}$, are shown together with the best fitting exponential continuum, for all different phase segments. In the lower panels: the same ratio divided by the continuum emphasizes the shape of the line. The line depth, width and centroid clearly depend on the pulse phase.